CP248, a Derivative of Exisulind, Causes Growth Inhibition, Mitotic Arrest, and Abnormalities in Microtubule Polymerization in Glioma Cells[1]

Jung-Taek Yoon, Alexander F. Palazzo, Danhua Xiao, Thomas M. Delohery, Peter E. Warburton, Jeffrey N. Bruce, W. Joseph Thompson, Gerhard Sperl, Clark Whitehead, John Fetter, Rifat Pamukcu, Gregg G. Gundersen, and I. Bernard Weinstein[2]

Herbert Irving Comprehensive Cancer Center [J-T. Y., D. X., I. B. W.], Department of Anatomy and Cell Biology [A. F. P., G. G. G.], Department of Neurological Surgery [J. N. B.], College of Physicians and Surgeons, Columbia University, New York, NY 10032; Flow Cytometry Core Facility, Memorial Sloan-Kettering Cancer Center, New York, New York 10021 [T. M. D.]; Department of Human Genetics, Mount Sinai School of Medicine, New York, New York 10029 [P. E. W.]; and Cell Pathways Inc., Horsham, Pennsylvania 19044 [W. J. T., G. S., C. W., J. F., R. P.]

Abstract

Exisulind (sulindac sulfone) and two potent derivatives, CP248 and CP461, have been shown previously to cause growth inhibition and apoptosis in several types of human carcinoma cell lines. These and related compounds have not been previously studied with respect to glioma cell lines. In the present study, we found that these three compounds caused marked growth inhibition in four rat glioma and eight human glioma cell lines, with IC_{50} values of 150, 1, and 0.075 μM, respectively. When studied at these concentrations exisulind and CP461 had no significant effect on the cell cycle profile of glioma cells, but CP248 caused marked arrest in mitosis. Detailed studies of CP248 in the 9L rat gliosarcoma cell line indicated that treatment with 0.075 μM CP248 caused abnormalities in the spindle apparatus and activation of the spindle assembly check point. In interphase glioma cells, CP248 stabilized microtubules (MTs) at low concentrations (0.075 μM) and depolymerized MTs at higher concentrations (0.2–0.4 μM). In NIH 3T3 fibroblasts, 0.1 μM CP248 caused extensive MT depolymerization. CP248 also caused MT depolymerization when added to assembled MTs *in vitro*, which indicated that it can directly affect MTs, perhaps because it shares certain structural similarities with Colcemid. In glioma cells, the effects of CP248 on MTs were independent of the previously reported effects of this compound on activation of protein kinase G. Therefore, CP248 is a novel MT-active agent that may be useful in the treatment of glioblastoma, and possibly other types of cancer, because of its dual effects on protein kinase G and MTs.

Introduction

GBM[3] are highly malignant tumors of the central nervous system. They are characterized by rapid growth, extensive vascularization and poor prognosis. Indeed, there is no curative treatment for these tumors. Resection is often the first line of treatment, followed by radiation therapy (1). Even with extensive radiation therapy and chemotherapy, the prognosis remains poor, with survival usually less than 1 year from the time of diagnosis. Therefore, it is desirable to develop more effective forms of therapy for this disease.

At present, there is considerable interest in the antitumor effects of various NSAIDs and derivatives of these drugs, especially with respect to colon cancer and other types of carcinomas. However, there are no detailed studies on the effects of these drugs on GBM. Therefore, in the present study we examined the effects of exisulind (sulindac sulfone), and two potent derivatives of exisulind, CP461 and CP248 (Fig. 1), on the growth of four rat glioma and eight human glioma cell lines. Exisulind was of particular interest because, although it does not inhibit COX1 or -2 (2), it inhibits the growth of polyps in patients with familial polyposis coli, prevents tumor formation in rodent models of carcinogenesis, and inhibits growth and induces apoptosis in several types of human cancer cell lines (3–6). CP461 and CP248 also lack COX1- and COX2- inhibitory activity, and induce apoptosis in human carcinoma cell lines, including prostate cancer cells, with potencies that are about 100- or 1000-fold greater, respectively, than exisulind (7). In the present study, we found that exisulind, CP248, and CP461 markedly inhibited the growth of four rat glioma and eight human glioma cell lines. We also found that, when tested at their IC_{50} concentrations, exisulind and CP461 had no significant effect on the

Received 2/19/02; accepted 2/19/02.
[1] Supported by awards from Cell Pathways, Inc., the T. J. Martell Foundation, and the National Foundation for Cancer Research (to I. B. W.). Additional grant support was from the American Cancer Society and NIH (to G. G. G.). A. F. P. was supported by a fellowship from the Fonds de la Recherche en Santé du Québec.
[2] To whom requests for reprints should be addressed, at Herbert Irving Comprehensive Cancer Center, College of Physicians and Surgeons, Columbia University, Columbia-Presbyterian Medical Center, 701 West 168th Street, Suite 1509, New York, NY 10032. E-mail: weinstein@cuccfa.ccc.columbia.edu.

[3] The abbreviations used are: GBM, glioblastoma(s) multiforme; NSAID, nonsteroidal anti-inflammatory drug; CP248, (*Z*)-5-flouro-2-methyl-1-(3,4,5-trimethoxybenzylidene)-3-(*N*-benzyl)-indenylacetamide; CP461, (*Z*)-5-flouro-2-methyl-(4-pyridylidene)-3-(*N*-benzyl)-indenylacetamide hydrochloride; COX, cyclooxygenase; MT, microtubule; MAP, MT-associated protein; KB+, buffer with Triton X-100; KB−, buffer without Triton X-100; MTOC, MT organizing center; cGMP, guanosine 3′,5′-cyclic monophosphate; PKG, protein kinase G; MPM-2, mitotic protein monoclonal (antibody); DAPI, 4′,6-diamidino-2-phenylindole; MAD, mitotic arrest-deficient.

cell cycle profile of these glioma cell lines, but CP248 caused the cells to arrest in M phase (mitosis).

MTs are cytoskeletal structures that play a critical role in the formation of the spindle apparatus during mitosis. They also play an important role in other biological processes including intracellular transport, exocytosis, signaling, maintenance of cell shape, and cell growth. MTs are formed of heterodimers of α- and β-tubulin and smaller amounts of MAPs. They undergo a dynamic process of polymerization and depolymerization. In addition, under certain conditions, a subset of MTs can be stabilized and thus polarize a cell, orienting its membrane and organelles (8–10). Certain cancer chemotherapy agents arrest cells in M phase by disrupting the dynamics of MT assembly. Thus, paclitaxel (Taxol) binds to and stabilizes MTs, whereas Colcemid and *Vinca* alkaloids bind to MTs and inhibit their polymerization. Thereby, these compounds perturb the function of the spindle apparatus (11–15).

Because CP248 caused cells to arrest in metaphase, we examined the effects of this drug on the spindle apparatus and on interphase MTs. We present evidence that CP248 can act directly to cause MT depolymerization, thereby disrupting the spindle apparatus and disorganizing the cytoskeleton. These novel effects of CP248 suggest that this compound, or related compounds, may be useful in the treatment of human GBM and possibly other types of refractory human malignancies.

Materials and Methods

Cell Lines and Cell Culture Conditions. The human glioma cell lines U87, A172, U373, and U138 and the rat glioma cell lines 9L and C6 were purchased from American Type Culture Collection. The rat glioma cell lines D74/RG1 and F98 were provided by Dr. R. F. Barth, Department of Pathology, Ohio State University, Columbus, OH (16). The human glioma cell lines GB1, GB2, GB3, and GB4 were established in the Bartoli Brain Tumor Laboratory of the Department of Neurosurgery, Columbia-Presbyterian Medical Center (New York, NY). All of the latter cell lines have been previously characterized and found to be positive for the glial specific protein, glial fibrillary acidic protein (GFAP), and negative for the neural markers MAP2 and neurofilament-160 (NF160). For additional descriptions of these cell lines, see Begemann *et al.* (17) and Venkatraj *et al.* (18). All of the cell lines were grown in DMEM (Life Technologies, Inc., Carlsbad, CA) supplemented with 10% calf serum (Life Technologies, Inc.), 100 units/ml penicillin and 100 μg/ml streptomycin (Life Technologies, Inc.). Cells were incubated in a 100% humidified incubator at 37°C with 5% CO_2. Exisulind (sulindac sulfone), CP461, and CP248 (Cell Pathways Inc., Philadelphia, PA) were diluted in DMSO. DMSO control assays contained 0.1% DMSO, the highest concentration of DMSO used with these drugs. Taxol was obtained from Dr. Ven L. Narayanan, National Cancer Institute, Bethesda, MA, and was used at a final concentration of 10 μM, as a positive control for the fluorescence microscopy studies. Colcemid (Roche, Indianapolis, IN) was also used at a final concentration of 50 ng/ml.

Thymidine Incorporation Assay. Cells were plated at 1×10^4 cells per well in 96-well plates and allowed to attach overnight. The cells were then treated with the indicated concentration of exisulind, CP461, or CP248, for 48 h. Tritiated thymidine (NEN, Boston, MA) was then added at 1 μCi/well. After 24 h the cells were washed twice with PBS, fixed with 100% methanol, washed with 10% trichloroacetic acid, and then with 70% ethanol. The fixed cells were then lysed with 10 N HCl, and neutralized with 10 N NaOH. Samples were collected in a 7 ml-scintillation vial and scintiverse (Fisher Scientific, Pittsburgh, PA) was added. Radioactivity was determined in a Beckman scintillation counter.

MPM-2 Staining for Cell Cycle Analysis. The 9L and human glioma cells were plated at a density of 6×10^4 and 2.5×10^5 cells per 100-mm dish, respectively, and allowed to grow for several days. When the cells were 60–80% confluent, they were treated with the IC_{50} concentrations (see Table 2) of CP248, CP461, or exisulind; 0.13 μM Colcemid; or 0.1% DMSO (solvent control). At the indicated time points, the cells were harvested via trypsinization (Life Technologies, Inc.) and washed twice with ice-cold PBS. The cells were then fixed with 70% ethanol and kept at 4°C until staining. The cells were pelleted and washed once with PBS and then with 2% FBS in PBS (staining buffer). They were then resuspended in 100 μl of staining buffer containing a 1:250 dilution of the MPM2 primary mouse antibody (Upstate Biotechnologies, Lake Placid, NY), and incubated at room temperature in the dark for 45 min. The cells were then washed twice with staining buffer and resuspended in 100 μl of staining buffer containing a 1:1000 dilution of a FITC-conjugated secondary goat antibody specific to mouse antibody (Rockland Immunochemicals for Research, Gilbertsville, PA) at room temperature for 45 min, in the dark. The cells at a concentration of 1×10^6 cells/ml were then washed twice with staining buffer and resuspended in 5 μg/ml propidium iodine (Sigma Chemical Co., St. Louis, MO) and 1 μg/ml RNase A (Sigma Chemical Co.). They were stored at 4°C for less than 1 week, until analyzed by flow cytometry.

Flow Cytometry and Cell Cycle Analysis. The DNA content of propidium iodide-stained cells was measured with a FACS Calibur instrument equipped with a FACstation and CellQuest software (Becton Dickinson, San Jose, CA). Cell cycle analyses of the DNA histograms were performed with the MultiCycle program (Phoenix Flow Systems, San Diego, CA).

Immunohistochemistry. Cells were grown on glass coverslips in 6-well plates. After the indicated exposures to the compounds (Figs. 2–5), the cells were washed once in PBS at 37°C and fixed with methanol at −20°C for 10 min. The fixed cells were then immunostained, essentially as described by Alonso *et al.* (19). Briefly, the fixed cells were washed three times with KB+ [10 mM Tris-HCl (pH 7.4), 0.15 M NaCl, 0.1% BSA, and 0.1% Triton X-100] for 10 min. Then the fixed cells were rinsed twice with KB− [10 mM Tris-HCl (pH 7.4), 0.15 M NaCl, and 0.1% BSA], and then washed twice in TEEN [1 mM Triethanolamine-HCl (pH 8.5), 0.2 mM EDTA, and 25 mM NaCl] for 10 min. The cells were then incubated with TEEN, 10% normal goat serum (Vector Labs, Burlingame, CA) plus the proper concentration of the primary antibody, as described below, for 1 h at 37°C, in a 100% humidified chamber. After incubation, the cells were washed

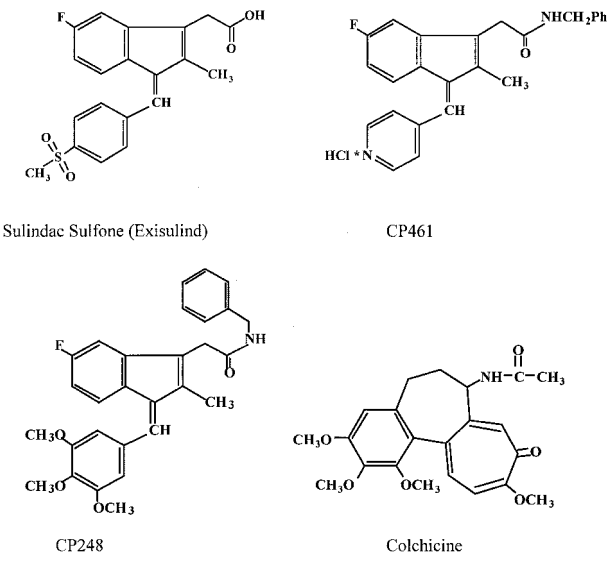

Fig. 1. Chemical structures of exisulind, CP461, CP248, and colchicine.

in the same manner as described above and exposed to TEEN, 10% normal goat serum plus the appropriate secondary antibody, as described below, for 45 min at 37°C in a 100% humidified chamber. The cells were then washed three times in KB+ for 10 min and then refixed in 4% formaldehyde in KB− for 10 min. Coverslips were then rinsed with tap water and mounted with Histomount (Vector Labs), and clear nail polish was used to seal the edges of the coverslip to the microscope slide.

Methanol-fixed cells were stained with DAPI at a 1:1000 dilution, to visualize DNA. MAD-2 was labeled with an anti-rabbit-MAD-2 antibody (Benezra; Memorial Sloan Kettering Cancer Center, New York, NY; Ref. 20) at a 1:200 dilution and then visualized with a goat antirabbit IgG-rhodamine conjugate (Chemicon International Inc., Temecula, CA), at a 1:100 dilution. The fixed cells were stained for MTs with the rat-YL1/2 (tyrosinated α-tubulin) antibody (21) at a 1:10 dilution of culture supernatant, and visualized with a goat antirat IgG-FITC conjugate (Chemicon International Inc., Temecula, CA) at 1:100 dilution. Rat YL1/2 hybridoma cells were purchased from the European Collection of Animal Cell Culture (Salisbury, United Kingdom). The cells were stained for stable MTs with rabbit antidetyrosinated tubulin antibody (SG; Ref. 22) at a 1:500 dilution, and visualized with a goat anti-rabbit IgG-rhodamine conjugate (Chemicon International Inc.). Centrosomes were labeled with a rabbit antipericentrin (23) antibody (Babco, Richmond, CA), at a dilution of 1:200, and visualized with a goat antirabbit IgG-Cy-5 conjugate (Chemicon International Inc.), at a 1:200 dilution.

MT Turbidity Assay. These assays were performed essentially as described by Schiff *et al.* (13). Briefly, turbidity was measured with a Hewlett Packard (model 8453) UV-Vis Spectrophotometer equipped with a thermostable chamber. MAP-rich tubulin (Cytoskeleton, Denver, CO) was diluted to 1 mg/ml in PEM [100 mM PIPES (pH 6.9), 1 mM EGTA, and 1 mM $MgCl_2$) buffer containing 1 mM GTP (GPEM), and kept on ice. This solution was then centrifuged at 100,000 $\times$ *g* (Beckman TL-100 Ultracentrafuge) for 7 min at 4°C, to remove aggregated tubulin. The supernatant fraction was then placed in a cuvette at 37°C, and absorbance was measured at 350 nm every 30 s. After 20 min, when polymerized tubulin had reached a steady state, 5 μM Taxol, 1.35 μM Colcemid, or 1 or 0.1 μM CP248 was added, and turbidity measurements were made for an additional 20 min.

Results

Inhibition of Cell Proliferation by Exisulind, CP461, and CP248. Table 1 summarizes the IC_{50} (concentration that inhibits growth by 50%) values obtained for growth inhibition of a series of four rat and eight human glioma cell lines by the compounds exisulind, CP461, and CP248, when assessed by [H^3]thymidine incorporation. The IC_{50} values for a given drug were remarkably similar among the 12 glioma cell lines, with values for exisulind of about 150 μM, for CP461 about 1 μM, and for CP248 about 0.07 μM.

Exisulind, CP461, and CP248 have been previously shown to inhibit cell proliferation in prostate (7), colon, and breast cancer cells lines,[4] with IC_{50} values similar or somewhat higher than those found with the glioma cells in the present study. Thus, glioma cells are quite sensitive to growth inhibition by these compounds. Of particular interest is the high potency of the compound CP248. Therefore, the remainder of the studies in this article focused on this compound.

CP248 Causes Mitotic Arrest in Glioma Cells. To determine possible effects of these compounds on cell cycle progression, exponentially dividing cultures of the 9L rat gliosarcoma and the GB1 human glioblastoma, cells were treated with 0.1% DMSO (vehicle control) or the IC_{50} concentration for growth inhibition (Table 1) of exisulind, CP461, or CP248 for 6, 12, or 24 h; and the cells were then analyzed by DNA flow cytometry. Conventional DNA flow cytometry does not distinguish cells that are in the G_2 phase of the cell cycle from those that are in the M phase (mitotic cells), because both types of cells have the same DNA content. Therefore, we performed DNA flow cytometry in conjunction with staining of the cells with a MPM antibody (MPM-2), which specifically stains phosphoproteins present only in mitotic cells (24–26). The results are summarized in Table 2. Exisulind- and CP461-treated 9L and GB1 cells did not display significant changes in their cell cycle profile when compared with DMSO-treated control cells. With the 9L cells, CP248 caused a slight increase in the number of cells in the G_2 phase. However, CP248 caused a marked increase in the mitotic index (*i.e.,* the percentage of cells in M phase), in both the 9L and GB1 glioma cell lines. Thus, in the 9L cell line, the mitotic index increased from 1.8 to 13.1% when cells were exposed to CP248 for 6 h, and to 15.7% after 12 h of treatment. In the CP248-treated GB1 cells, the mitotic index increased from 2.2 to 9.9% at 12 h and from 2.4 to 16.4% after 24 h. Therefore, there was about an 8-fold or a 7-fold

[4] Unpublished observations.

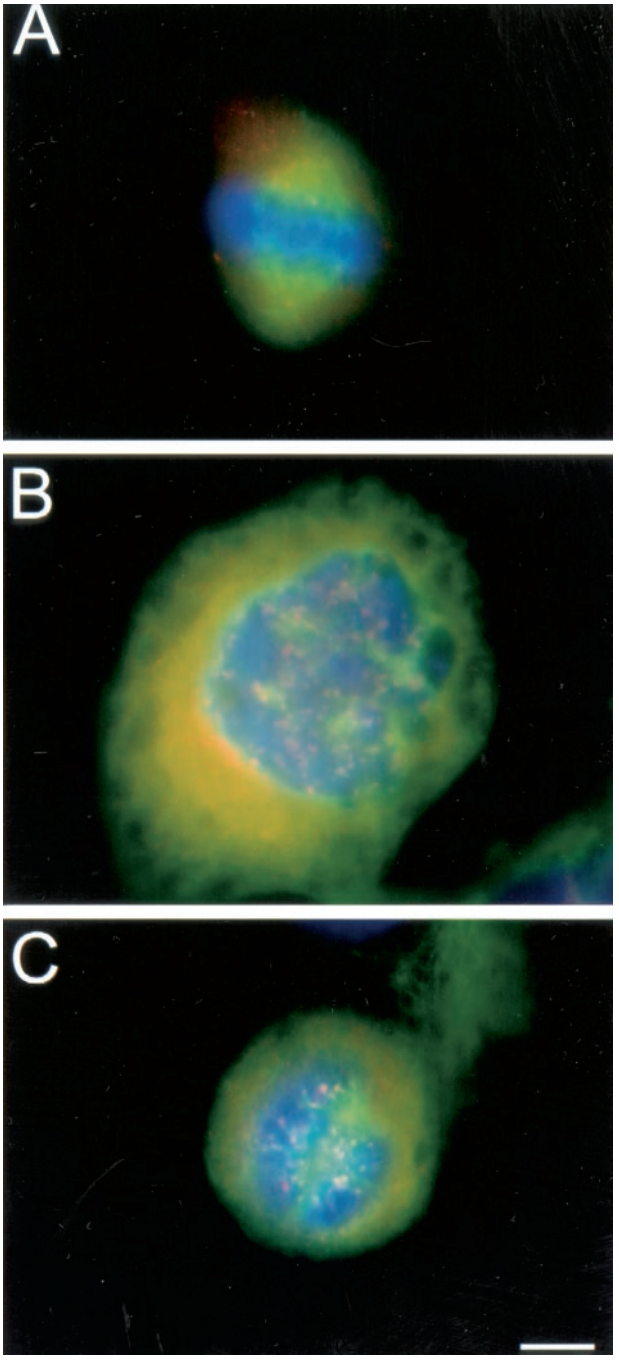

Fig. 2. Effects of CP248 on mitotic 9L cells. *A*, a mitotic 9L cell after treatment with 0.1% DMSO (solvent control). *B*, a 9L cell treated with 50 ng/ml Colcemid (positive control). *C*, a mitotic 9L cell after treatment with 0.075 μM CP248. Cells were treated for 12 h and fixed with methanol. Chromosomal DNA was *stained blue* with DAPI. MTs were *stained green* and MAD2 proteins were *stained red* with the respective antibodies and were visualized by indirect immunofluorescence, as described in "Materials and Methods." Abnormal spindle apparatus is notable in the CP248-treated cells. *White bar*, 10 μm.

increase in the mitotic index for the 9L and the GB1 cells, respectively. The more rapid effect on the arrest in mitosis in the 9L *versus* the GB1 cells is consistent with the more rapid doubling time of the 9L cells. We also tested the effects of Colcemid (0.13 μM) on GB1 cells. This provided a positive control, because this concentration of Colcemid is known to cause mitotic arrest (14). We found that under these conditions the mitotic arrest produced by CP248 on GB1 cells was even greater than that produced by Colcemid (Table 2). These results indicate that CP248, when added at its IC_{50} concentration, causes a major fraction of the 9L and GB1 cells to arrest in mitosis. Similar results were obtained with CP248 and the GB2 human glioma cell line (data not shown).

After more prolonged treatment with CP248, the fraction of 9L cells arrested in M phase declined from 15.7 to 4.4% for the 12 and 24 h time points, respectively, after the addition of CP248 (Table 2). This was associated with an increase, from 7 to 17.4%, in the fraction of cells that had a greater amount of DNA than the G_2 amount (Table 2). The latter result appears to be attributable to endoreduplication, *i.e.,* the process by which mitotic cells fail to undergo cytokinesis but, nevertheless, proceed to another round of DNA synthesis, thus further increasing the amount of DNA per cell (27). Similar findings were seen at 24 h with Colcemid, a known inhibitor of mitosis (data not shown). Therefore, although CP248 causes glioma cells to arrest in the M phase, this cell cycle arrest is not complete, possibly because of deficient mitotic checkpoint control in these cancer cells.

The Spindle Assembly Checkpoint Is Activated in CP248-treated Cells. In view of the ability of CP248 to arrest glioma cells in mitosis, we examined possible effects of this compound on the spindle assembly checkpoint, in 9L and GB2 cells. The human MAD2 protein, cloned by Li and Benezra (20), plays an important role in the spindle assembly checkpoint (28–30). MAD2 acts in concert with a group of proteins that regulate progression through mitosis, thus assuring the proper segregation of sister chromosomes to each daughter cell (31, 32). When cells are defective in mitosis, MAD2 remains bound to the kinetochores (33), so that there is an increase in the fraction of chromosomes that are MAD2-positive.

We used immunofluorescent microscopy to detect the presence of MAD2 on cellular kinetochores. A representative result obtained when 9L cells were treated with CP248 for 12 h is shown in Fig. 2*C*, in which MAD2 is displayed in *red* and chromosomes in *blue*. Treatment with CP248 (Fig. 2*C*) increased the number of mitotic cells with MAD2 staining when compared with DMSO-treated cells (Fig. 2*A*). We then did a quantitative study with GB2 cells in which we determined by microscopy the percentage of cells in mitosis that displayed increased expression of MAD2. Colcemid-treated cells were used as a positive control to display MAD2 expression when the spindle assembly is disrupted as a result of inhibition of tubulin polymerization (Fig. 2*B*). The quantitative results are summarized in Table 3. In the untreated control cells, 18% of the mitotic cells were positive for MAD2. Similar results were obtained in cells treated with exisulind or CP461. When, however, the cells were treated with CP248, 58% of the mitotic cells were positive, and when the cells were treated with Colcemid, 98% of the cells were positive, for increased expression of MAD2 (Table 3). In addition, we observed abnormal spindle formations in the

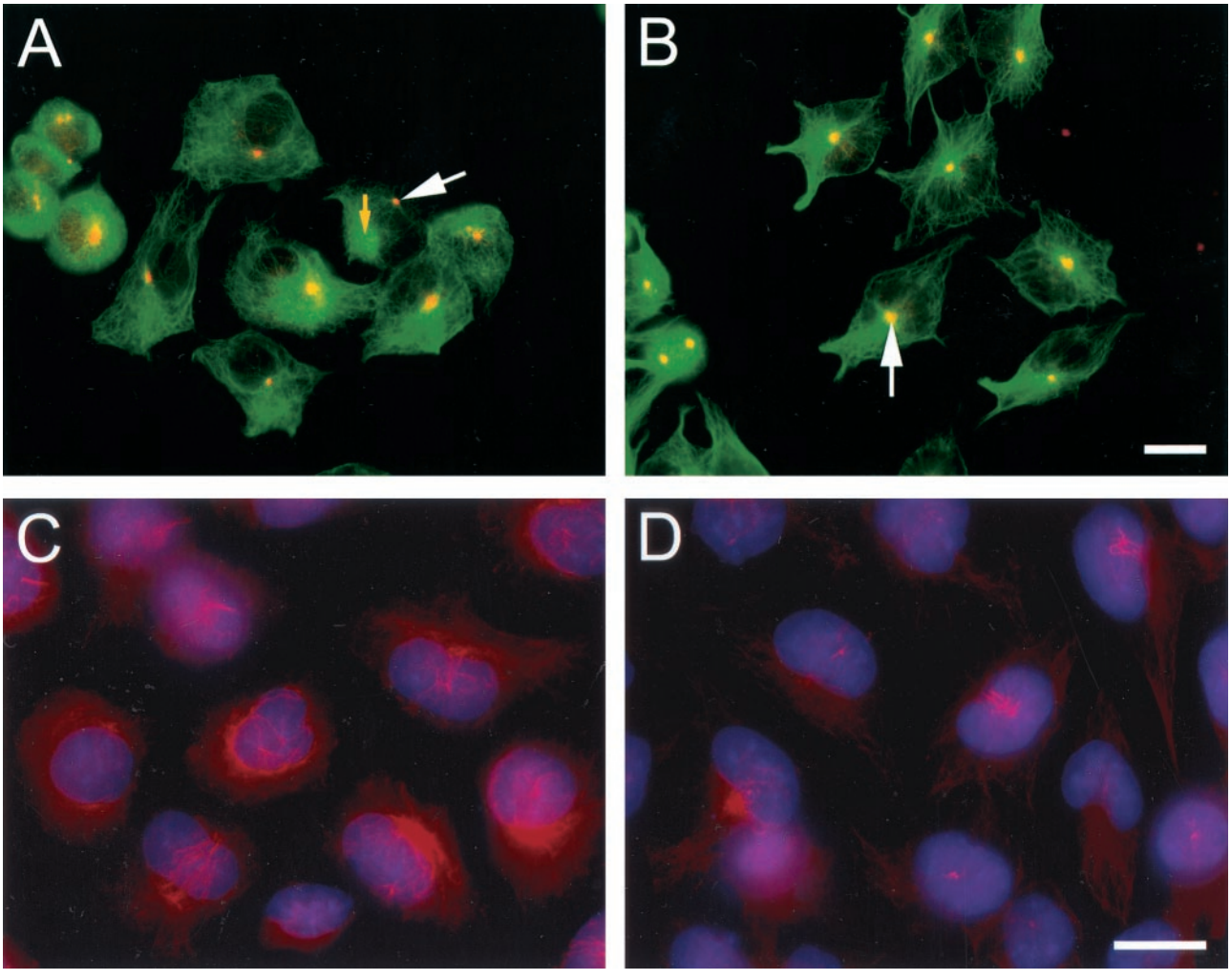

Fig. 3. Effects of CP248 on interphase 9L cells. The 9L cells were treated with 0.075 μM CP248 (*A*, *C*) or 0.1% DMSO (*B*, *D*) for 6 h, fixed with methanol; and DNA, MTs, and centrosomes were visualized by indirect immunofluorescence, as described in Fig. 2 and "Materials and Methods." In *B*, DMSO-treated 9L cells show a tight correlation of centrosomes (*stained red*) with the MT array (*white arrow*). In *A*, CP248-treated 9L cells show a dissociation of the centrosome (*white arrow*) from the MT array (*yellow arrow*). In *C*, CP248-treated 9L cells were stained for stable Glu MTs (*red*) and DNA (*blue*). In *D*, DMSO-treated 9L cells were stained for stable Glu MT (*red*) and for DNA (*blue*). *White bars*, 20 μm.

CP248-treated mitotic 9L cells (Fig. 2*C*), when these cells were compared with the untreated 9L cells (Fig. 2*A*). Taken together, these findings suggested that cells treated with CP248 arrest in mitosis because of abnormalities in the formation of the spindle apparatus, and that this leads to activation of the spindle assembly checkpoint.

Abnormalities in MT Organization in CP248-treated Cells Which Cause Defects in the Formation of the Spindle Apparatus. Taxol and Colcemid arrest cells in metaphase by interfering with MT polymerization, thereby impairing the spindle apparatus. These drugs also perturb MT polymerization in interphase cells (34). Therefore, we examined whether CP248 also caused abnormalities in MT polymerization or organization in interphase 9L cells. As expected, in the control DMSO-treated interphase 9L cells, the MTs were organized in a radial array with the centrosome at the focus of the MT-minus ends (Fig. 3*B*, *white arrow*). However, in 9L cells treated with 0.075 μM CP248, MTs were not in a radial array and many of the centrosomes (Fig. 3*A*, *stained red*, *white arrow*) appeared to be separated from the bulk of the MTs (Fig. 3*A*, *yellow arrow*). Therefore, when studied at its IC_{50} concentration for growth inhibition, CP248 can disrupt the normal organization of MTs in interphase 9L cells.

CP248 at Low Concentrations (0.075 μM) Stabilizes MTs in 9L Cells. The separation of the bulk of the MTs from the centrosome in cells treated with the IC_{50} concentration of CP248 was unusual and suggested that CP248 might cause stabilization of MTs. To test whether CP248 at its IC_{50} concentration induces MT stability, we immunostained the treated cells with an antibody to detyrosinated (Glu) tubulin. When stabilized MTs are present in cells for long durations, the polymerized tubulin becomes a substrate for the enzyme tubulin carboxy-peptidase, which cleaves the COOH-terminal tyrosine residue, thus leaving the tubulin with a glutamate residue at its COOH-terminal end (22). This "Glu tubulin"

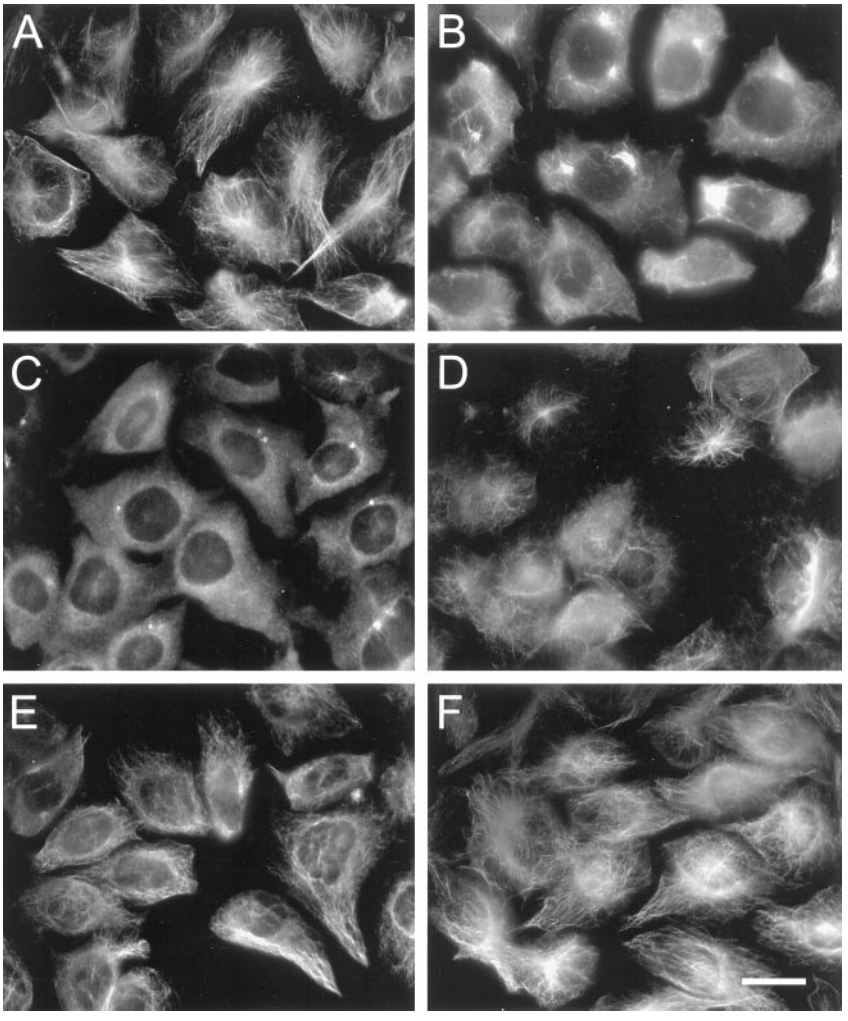

Fig. 4. Effects of CP248 on MTs in interphase 9L cells. 9L cells were treated with 0.1% DMSO (*A*), 0.2 μM CP248 (*B*), or 0.4 μM CP248 (*C*) for 2 h. The cells were fixed with methanol, and MTs were visualized by immunofluorescence, as described in "Materials and Methods." The 9L cells were treated with 0.4 μM CP248 for 2 h, washed three times with fresh medium, and then incubated for an additional 15 (*D*), 30 (*E*), or 60 (*F*) min, before fixation and immunostaining. *White bars*, 20 μm.

accumulates in a small subset of MTs that have been stabilized (35, 36). These so-called "stable MTs" appear in differentiated cells and in polarized cells (8). Therefore, we used a specific antibody that recognizes the detyrosinated form of tubulin (22) to detect, by immunostaining, stabilized MTs in 9L cells.

Fig. 3, *C* and *D*, display 9L cells stained for stable MTs (*stained red*) and DNA (*stained blue*). In untreated 9L cells (Fig. 3*D*), we observed a small amount of stable MTs, but stable MTs were markedly increased in cells treated with 0.075 μM CP248 (Fig. 3*C*). We next quantified by microscopy the number of cells that expressed stable MTs (Table 4). In 9L cells treated with 0.075 μM CP248, 44% of the cells contained 12 or more stable MTs, whereas in the untreated cells, this value was 22%. Thus, when tested at its IC_{50} concentration (0.075 μM) CP248 stabilizes MTs in 9L cells.

CP248 at High Concentrations (0.2–0.4 μM) Causes MT Depolymerization in 9L Cells. As described above, when tested at 0.075 μM, CP248 altered the normal organization of MTs in 9L glioma cells (Figs. 2*C* and 3*A*) and induced MT stability (Fig. 3*C*). Other MT-depolymerizing agents, such as Colcemid, vinblastin, and nocodozole, dampen MT dynamics at low concentrations that block mitosis but are potent depolymerizing agents at higher concentrations. In view of these dose-dependent effects, we examined the effects of higher concentrations of CP248 on MTs in 9L cells. Indeed, we found that when 9L cells were treated with 0.2 μM CP248 for 2 h, we observed depolymerization and fragmentation of MTs (Fig. 4*B*), and when treated for 2 h with 0.4 μM CP248, we observed complete depolymerization of MTs (Fig. 4*C*). If 9L cells were treated with 0.4 μM CP248 for 2 h, and then washed free of the drug, MTs began to reappear within 15 min (Fig. 4*D*), increased at 30 min (Fig. 4*E*), and at 1 h appeared to reform a normal array (Fig. 4*F*). Therefore, treatment of 9L glioma cells with higher concentrations of CP248 (0.2–0.4 μM) causes complete depolymerization of MTs, and this effect is rapidly reversible when the cells are washed free of CP248.

CP248 Depolymerizes MTs in Serum-starved NIH 3T3 Fibroblasts. We also examined the effects of CP248 on serum-starved NIH 3T3 mouse fibroblast cells because this is a well-characterized model system for examining MT stability (37). As previously described (37, 38), when starved of serum, these fibroblasts expressed very few stable MTs (not

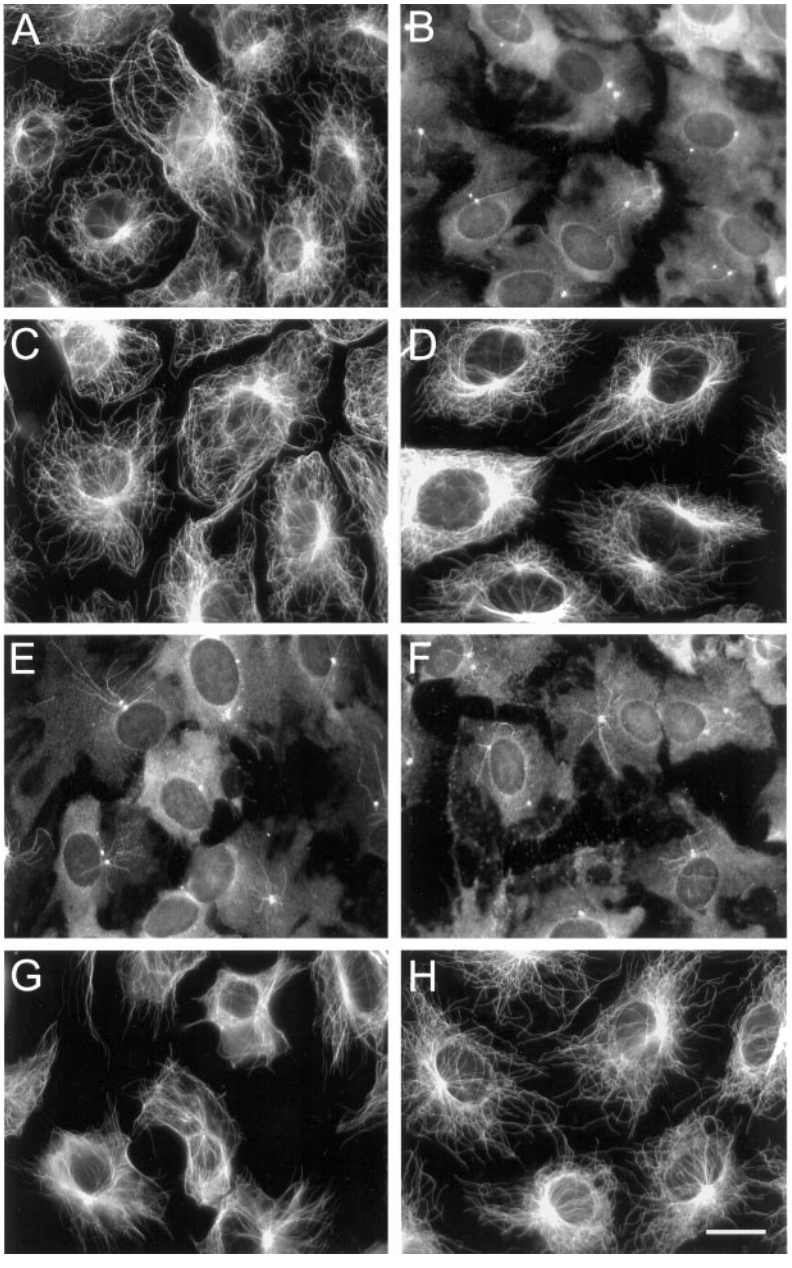

Fig. 5. Effects of CP248 on MTs in NIH 3T3 fibroblasts. The cells were grown in medium in the absence of serum for 48 h. They were then incubated in medium minus serum containing: 0.1% DMSO (*A*); 0.1 μM CP248 (*B*); 200 μM exisulind (*C*); 1.5 μM CP461 (*D*); 0.1 μM CP248 plus 10 μM KT5823 (*E*); 0.1 μM CP248 plus 10 μM Rpt-8-pCPT0cGMP (*F*); 170 nM YC-1 (*G*); or 4 mM dibutyryl cGMP (*H*). After 2 h of incubation with these agents, the cells were fixed with methanol and the MTs visualized by immunofluorescence, as described in "Materials and Methods." *White bars*, 20 μm.

shown) and a normal array of MTs (Fig. 5*A*). We found that the IC_{50} for inhibition of proliferation of the fibroblast cells by CP248 was 0.1 μM (Table 1). When serum-starved fibroblasts were treated with this concentration of CP248, we found that normal dynamic polymerized MTs were no longer present in these cells (Fig. 5*B*), and the few MTs that were still present were stable MTs.

Possible Roles of cGMP and PKG Activation in MT Depolymerization. Recent studies indicate that in human colon cancer cells, exisulind, CP248, and related compounds induce apoptosis by inhibiting cGMP-specific phosphodiesterases 2 and 5, thereby increasing cellular levels of cGMP and activating PKG, which then causes apoptosis (39, 40). Similar results have been obtained with NIH 3T3 mouse fibroblast cells.[5] Therefore, it was of interest to determine whether this pathway plays a role in the effects of CP248 on MTs. Fig. 5*A* shows that serum-starved fibroblasts treated only with the DMSO solvent, displayed a normal array of MTs. Fig. 5*B* indicates that, when serum-starved fibroblasts were exposed to 0.1 μM CP248 for 2 h, virtually all of the MTs were depolymerized. When serum-starved fibroblasts were exposed to IC_{50} concentrations of exisulind (Fig. 5*C*) or CP461 (Fig. 5*D*), we did not see the extensive depolymerization of MTs seen with CP248. Therefore, under these conditions, CP248 differs from exisulind and CP461 in its

[5] Unpublished observations.

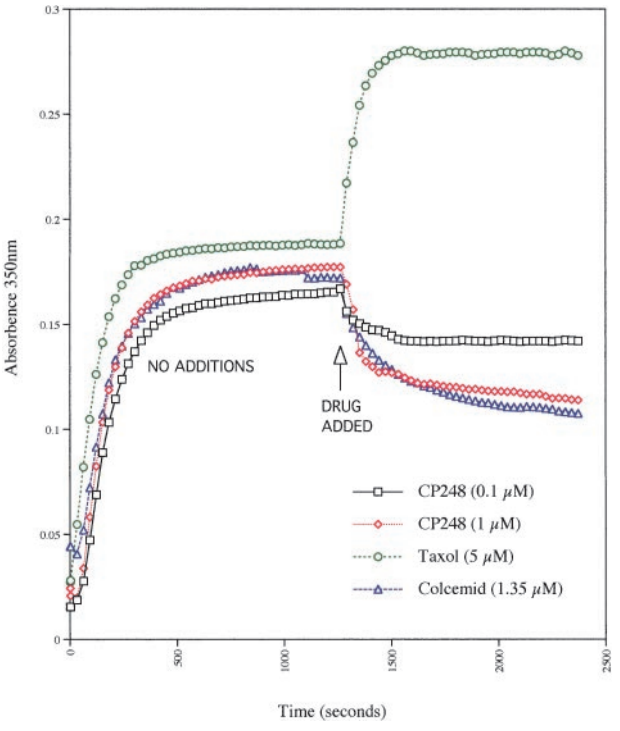

Fig. 6. Effects of CP248 on *in vitro* MT polymerization, measured by turbidity. A solution of MTs at 4°C was placed into a thermostable chamber of a spectrophotometer and incubated at 37°C. Absorbance at 350 nm was then determined during the indicated time course. After MT polymerization reached a steady state (20 min), 5 μM Taxol, 0.1 μM CP248, 1 μM CP248, or 1.35 μM Colcemid were added. Because Colcemid and CP248 gave some absorbance at 350 nm, this value was subtracted from the total absorbance. For additional details, see "Materials and Methods."

Table 1 Inhibition of cell proliferation by sulindac sulfone (exisulind) and derivatives in a series of glioma cell lines

Cell proliferation was determined by tritiated thymidine incorporation, as described in "Materials and Methods." IC_{50} values, calculated from a concentration curve, indicate the concentrations of the drugs that caused a 50% inhibition of tritiated thymidine incorporation when compared with a control culture treated only with the vehicle, 0.1% DMSO. Data are the mean values from two separate experiments in which all of the assays were done in triplicate. Repeat assays differed by less than 10%.

Cell line	IC_{50} (μM)		
	Exisulind	CP461	CP248
Rat glioma cell lines			
9L	179	1.14	0.078
C6	168	1.08	0.068
F98	96	0.725	0.075
D74	137	1.02	0.064
Human glioma cell lines			
U87	140	1.43	0.083
U138	140	1.19	0.070
U373	145	0.98	0.077
A172	135	1.17	0.078
GB1	240	0.8	0.069
GB2	180	1.35	0.073
GB3	172	1.04	0.067
GB4	145	1.09	0.088
NIH mouse fibroblasts			
3T3	200	1.5	0.108

ability to cause MT depolymerization in serum-starved fibroblasts.

When serum-starved fibroblasts were exposed to CP248 in the presence of the PKG inhibitors KT5823 (10 μM, Fig. 5*F*) or RP-8-pCPT-cGMP (10 μM, Fig. 5*E*), we still observed MT depolymerization. We found that the addition of YC-1 (170 nM), which increases cellular levels of cGMP by stimulating guanylyl cyclase (41), to serum-starved fibroblasts did not lead to the loss of MTs seen with CP248. The MTs in the YC-1-treated 3T3 fibroblasts were, however, somewhat abnormal because they were straighter (Fig. 5*G*) than the MTs in the control, untreated 3T3 fibroblasts (Fig. 5*A*). The addition of 4 mM dibutyryl-cGMP to serum-starved fibroblasts had no detectable effect on the MTs (Fig. 5*H*), nor did 0.5, 1, or 2 mM dibutyryl-cGMP (data not shown). Taken together, these results suggest that the effects of CP248 on MTs in serum-starved fibroblasts are not mediated by an increase in cellular levels of cGMP or by activation of PKG.

CP248 Causes Direct Depolymerization of MTs When Tested *in Vitro*. To determine whether CP248 has a direct effect on tubulin polymerization, we performed *in vitro* MT assembly assays by measuring the turbidity of MTs formed from a population of MT proteins which contains both tubulin and MAPs. The suspension of MT protein was incubated at 37°C for 20 min, when turbidity indicated that tubulin polymerization had reached a plateau, and then the test compounds were added. As expected (13, 42), the addition of 5 μM Taxol caused increased tubulin polymerization, whereas the addition of 1.35 μM Colcemid caused decreased tubulin polymerization (Fig. 6). The addition of 0.1 μM CP248 caused a decrease, and the addition of 1 μM CP248 caused a marked decrease, in tubulin polymerization. Indeed, the latter effect was similar to that produced by 1.35 μM Colcemid (Fig. 6). We also found that CP248 caused a decrease in tubulin polymerization when we used a pure preparation of tubulin (data not shown). Therefore, it appears that the ability of CP248 to cause MT depolymerization in intact serum-starved fibroblasts and in glioma cells is caused by a direct effect on tubulin, rather than an indirect cell-mediated effect.

Discussion

Although several NSAIDs and the sulindac metabolite exisulind (sulindac sulfone) have been extensively studied for their antitumor effects in various types of carcinoma cells (reviewed in Refs. 40, 43, 44), this paper provides the first evidence that agents in this broad category of compounds are active as growth inhibitors of glioma cells. Indeed, we found that exisulind and two potent derivatives, CP461 and CP248, inhibited the growth of four rat glioma and eight human glioma cell lines with IC_{50} values of 150, 1, and 0.07 μM, respectively (Table 1). These concentrations are similar to, or less than, those required to inhibit human colon or prostate carcinoma cell lines. Our results suggest that these compounds, when used alone or in combination with other drugs, might be useful in the treatment of patients with gliomas. This is of particular interest because, as discussed in the "Introduction," malignant glioblastomas are usually refractory to conventional chemotherapy.

Table 2 Flow cytometric analysis

Cell cycle analysis was performed as described in "Materials and Methods." Cells were treated with the indicated compounds at their respective IC_{50} values (see Table 1), collected at the indicated time points, and analyzed by DNA flow cytometry. The values obtained are an average of two independent experiments, with a minimum of 15,000 events collected for each time point. Duplicates agreed within 5%.

Treatment	6 h (%)	12 h (%)	24 h (%)
9L cell line			
No treatment			
G_0-G_1	46.1	48.4	52.7
S	32.7	36.1	32.0
G_2	**19.3**	**13.8**	**13.8**
M	**1.8**	**1.8**	**1.6**
>G_2-M	3.9	2.9	3.5
CP248 (0.078 μM)			
G_0-G_1	27.2	31.8	32.8
S	35.2	28.4	42.4
G_2	**24.5**	**24.2**	**20.5**
M	**13.1**	**15.7**	**4.4**
>G_2-M	4.0	7.0	17.4
CP461 (1.14 μM)			
G_0-G_1	44.4	44.6	55.4
S	33.5	36.9	30.0
G_2	**19.7**	**15.9**	**12.7**
M	**2.4**	**2.7**	**1.9**
>G_2-M	2.6	2.7	2.3
Exisulind (180 μM)			
G_0-G_1	48.8	50.7	58.4
S	30.2	34.5	28.8
G_2	**19.5**	**13.2**	**11.5**
M	**1.6**	**1.7**	**1.3**
>G_2-M	2.1	2.3	2.4
GB1 cell line			
No treatment			
G_0-G_1	47.5	54.7	38.0
S	17.8	13.9	30.9
G_2	**32.7**	**29.2**	**28.7**
M	**2.0**	**2.2**	**2.4**
>G_2-M	8.7	6.4	9.4
CP248 (0.07 μM)			
G_0-G_1	44.1	42.5	21.1
S	18.7	17.3	30.4
G_2	**32.9**	**30.3**	**32.1**
M	**4.9**	**9.9**	**16.4**
>G_2-M	8.5	8.8	11.7
CP461 (0.8 μM)			
G_0-G_1	48.7	54.2	38.1
S	19.0	14.7	30.2
G_2	**29.1**	**27.5**	**28.3**
M	**2.3**	**3.7**	**3.4**
>G_2-M	7.5	6.5	9.7
Exisulind (24 μM)			
G_0-G_1	47.9	53.7	49.0
S	19.2	14.1	24.8
G_2	**31.2**	**29.8**	**24.3**
M	**1.8**	**2.4**	**2.0**
>G_2-M	7.8	7.4	7.1
Colcemid (0.13 nM)			
G_0-G_1	41.6	42.4	11.8
S	19.7	13.8	42.0
G_2	**37.1**	**38.4**	**35.8**
M	**1.7**	**3.9**	**10.4**
>G_2-M	9.9	10.1	13.6

Table 3 MAD2 expression

The human glioma cell line GB2 was treated with CP248, CP461, or exisulind at the respective IC_{50} concentrations for 18 h and immunostained for MAD2, as described in "Materials and Methods." MAD2 overexpression was defined as the percentage of mitotic cells in which >50% of the chromosomes stained positive for MAD2. An example is shown in Fig. 2*C*. Mitotic cells on a single glass coverslip were scored for MAD2 expression by microscopy with a ×100 Nikon objective. More than 150 mitotic cells were scored for each of the treatment conditions.

Drug	GB2 Mad2 overexpression	
	(%)	(SD)
No drug	18	0
Colcemid	98	2.4
CP248	58	5.7
CP461	20	1.4
Exisulind	18	1.4

Table 4 Effects of the IC_{50} concentration of CP248 on stabilized MT in 9L cells

The 9L cells were treated with the IC_{50} concentration of CP248 for 6 h, fixed, and stained for stable MT with the SG antibody, as described in "Materials and Methods" and Figs. 3, *C* and *D*. A positive cell was defined as any cell that expressed 12 or more SG-stained MT or very bright foci of SG. Bright foci of SG represent a large amount of stabilized MT in a concentrated region of the cell. This experiment was repeated twice with similar results. A minimum of 150 cells were scored in each experiment.

Drug	% of cells positive	SD
None	21.85	±0.9
CP248	43.85	±10.4

In the present study, CP248 was of particular interest, not only because of its extreme potency as a growth inhibitor but because it caused cells to arrest in the M phase of the cell cycle, *i.e.,* in mitosis (Table 2). The latter effect was not confined to glioma cells, because we have also seen this effect in human prostate and colon cancer cell lines (Ref. 7 and unpublished studies).[6] More detailed studies indicated that 9L rat glioma cells treated with 0.075 μM CP248 displayed disruptions of the spindle apparatus (Fig. 2). There was also an increase in the fraction of mitotic cells that stained positive for the MAD2 protein (Fig. 2; Table 3), providing evidence that treatment with CP248 resulted in activation of the spindle assembly checkpoint. These effects were not seen when 9L glioma cells were treated with the IC_{50} concentrations of the drugs exisulind or CP461 (data not shown).

The cytological abnormalities produced by CP248 were not confined to mitotic cells, because when we examined the cytoplasm of 9L cells in interphase, we found that treatment with 0.075 μM CP248 resulted in dissociation of the MT array from its usual association with the centromere (Fig. 3). With this concentration of CP248 we also observed an increase in stable MTs in interphase 9L cells (Fig. 3*C*). However, when 9L cells were treated with a higher concentration of CP248 (0.4 μM), we found complete depolymerization of the dynamic

[6] Unpublished observations.

MTs (Fig. 4*C*). Taken together, these findings suggest that, like colchicine, Colcemid, and nocodozole (45), CP248 causes glioma cells to arrest in mitosis because it causes abnormalities in the polymerization of MTs. Therefore, the type of effect of CP248 on MT polymerization in 9L glioma cells appears to be concentration dependent. The MT-depolymerizing effects seen at higher concentrations resemble the effects of the extensively studied MT-depolymerizing agents colchicine, Colcemid, vinblastin, and nocodazole (45). On the other hand, the addition to interphase cells of Taxol causes MT polymerization (45). In mitotic cells, MT dynamics can be up to 20 times greater than in interphase cells. Therefore, low concentrations of either MT-depolymerizing or MT-stabilizing agents can cause mitotic arrest. Low concentrations of nocodazole or vinblastin dampen MT turnover at the positive ends of MTs (11, 45, 46). In glioma cells, low concentrations of CP248 may cause stabilization of MTs by dampening MT dynamics.

To further examine the effects of CP248 on MT depolymerization, we used NIH 3T3 fibroblasts, because they have a more highly organized cytoskeleton than glioma cells. Furthermore, Gundersen *et al.* (37) have shown that, when these cells are starved of serum, they display a well-defined array of MTs. Therefore, this provides a valuable model system for studying the effects of various agents on MTs. When we added a relatively low concentration of CP248 to serum-starved NIH3T3 fibroblasts, *i.e.,* 0.1 μM (which is the IC_{50} value for CP248-induced growth inhibition of these cells), there was extensive MT depolymerization (Fig. 5). Thus, CP248 can induce MT depolymerization in both malignant glioma cells and nontransformed fibroblasts, although higher concentrations of this drug are required in the glioma cells. In future studies, it will be of interest to examine the effects of a range of concentrations of CP248 on MT polymerization in other types of cells, both normal and malignant.

Although an increase in cellular levels of cGMP and activation of PKG have been implicated in the induction of apoptosis in cancer cells (40), these changes do not appear to mediate the effects of CP248 on MT polymerization, because treatment of 3T3 fibroblasts with dibutyryl-cGMP or YC-1, an activator of guanyl cyclase, did not cause MT depolymerization (Fig. 5*G*). Furthermore, treatment of these cells with the inhibitors of PKG KT5823 or RP-8-pCT-cGMP did not block the ability of CP248 to cause MT depolymerization (Fig. 5F and E). Therefore, in these cells, CP248 appears to exert its effects on MTs by a mechanism independent of its effects on cGMP and PKG. Consistent with this conclusion are our findings, discussed below, that CP248 can interact directly with tubulin.

We examined the possibility that, like Colcemid (42), CP248 might bind directly to tubulin and, thereby, depolymerize MTs. Indeed, using a standard *in vitro* turbidity assay for tubulin polymerization, we found that, like Colcemid, CP248 had a direct depolymerizing effect on tubulin (Fig. 6). As expected (13), Taxol had the opposite effect, *i.e.,* it increased tubulin polymerization. The concentrations of CP248 used in these *in vitro* studies are higher than those used in our cell-based assays. However, one cannot make direct dosage comparisons, because of the arbitrary concentration of tubulin and the other reaction conditions used in these *in vitro* turbidity assays. In addition, with the other MT-depolymerizing drugs, higher concentrations are also required in this *in vitro* assay than in cell-based assays. Although in the studies described in Fig. 6, we used a MT-rich preparation of tubuliln, similar results have been obtained with a pure preparation of tubulin (data not shown). Therefore, it appears that CP248 interacts directly with tubulin.

The *A* ring of colchicine consists of a trimethoxyphenyl group that plays a role in its binding to tubulin (47). It is of interest that CP248, but not exisulind or CP461, also contains a trimethoxyphenyl group (Fig. 1). Therefore, this structural feature may help to explain why CP248 can inhibit tubulin polymerization. Indeed in unpublished studies we have found that CP248 competes with colchicine for *in vitro* binding to a purified preparation of tubulin.[7] Recent studies indicate that the *C* ring of colchicine also plays a role in the binding of this drug to tubulin (47). Additional studies are required to determine the additional structural features of CP248 that are required for its effects on tubulin polymerization. The binding of CP248 to tubulin appears to be reversible because, when 9L glioma cells were exposed to the drug for 2 h and then the drug was removed from the medium, MTs began to reform within 15 min, and the cells displayed a normal array of MTs within one h (Fig. 4). Similar reversible effects have been seen with the colchicine analogue 2-methoxy-5-(2′,3′,4′-trimethoxyphenyl)-2,4,6-cycloheptatrien-1-one (MTC; Ref. 48) and nocodazole. As described above, in 9L cells, a low concentration (0.075 μM) of CP248 caused an increase in stable MTs, whereas higher concentrations (0.2–0.4 μM) caused MT depolymerization (Figs. 3*E* and 4, *B* and *C*). A possible explanation for these reciprocal effects is that, at substoichiometric conditions, CP248 preferentially binds to the ends of MTs, thereby dampening MT dynamics and increasing the fraction of stable MTs.

Taken together, the above studies suggest that CP248 is unique as an inhibitor of tumor cells because it appears to have two distinct biological functions. The first is the previously described ability to directly inhibit the cGMP-specific phosphodiesterases 2 and 5, and, thereby, activate a PKG-mediated signaling pathway that triggers apoptosis (39, 40). The second is the ability of CP248 to bind directly to tubulin and to thereby perturb MT polymerization and the function of the spindle apparatus, which causes cells to arrest in mitosis. In view of these dual effects, CP248, or related compounds, might be particularly effective in the treatment of patients with glioblastoma, or other types of cancer that are refractory to current forms of chemotherapy.

Acknowledgments

We thank Dr. Robert Benezra (Memorial Sloan-Kettering Cancer Center, New York, NY) for his generous gift of the MAD2 antibody. We thank Dr. Anna Marie Pyle (Columbia University, New York, NY) for the use of the thermostable spectrophotometer.

[7] Unpublished observations.

Note added in proof

In recent unpublished studies, we found that both CP248 and CP461, but not exisulind, can induce mitotic arrest in SW480 human colon cancer cells.

References

1. Fetell, M. R. Gliomas. *In:* L. P. Rowland (ed.), Merritt's Textbook of Neurology, Ed. 9, pp. 336–351. Baltimore, MD: Williams & Wilkins, 1995.

2. Piazza, G. A., Alberts, D. S., Hixson, L. J., Paranka, N. S., Li, H., Finn, T., Bogert, C., Guillen, J. M., Brendel, K., Gross, P. H., Sperl, G., Ritchie, J., Burt, R. W., Ellsworth, L., Ahnen, D. J., and Pamukcu, R. Sulindac sulfone inhibits azoxymethane-induced colon carcinogenesis in rats without reducing prostaglandin levels. Cancer Res., *57:* 2909–2915, 1997.

3. Moorghen, M., Ince, P., Finney, K. J., Sunter, J. P., Appleton, D. R., and Watson, A. J. A protective effect of sulindac against chemically-induced primary colonic tumours in mice. J. Pathol., *156:* 341–347, 1988.

4. Giardiello, F. M., Hamilton, S. R., Krush, A. J., Piantadosi, S., Hylind, L. M., Celano, P., Booker, S. V., Robinson, C. R., and Offerhaus, G. J. Treatment of colonic and rectal adenomas with sulindac in familial adenomatous polyposis. N. Engl. J. Med., *328:* 1313–1316, 1993.

5. Chiu, C. H., McEntee, M. F., and Whelan, J. Sulindac causes rapid regression of preexisting tumors in Min/+ mice independent of prostaglandin biosynthesis. Cancer Res., *57:* 4267–4273, 1997.

6. Beazer-Barclay, Y., Levy, D. B., Moser, A. R., Dove, W. F., Hamilton, S. R., Vogelstein, B., and Kinzler, K. W. Sulindac suppresses tumorigenesis in the Min mouse. Carcinogenesis (Lond.), *17:* 1757–1760, 1996.

7. Lim, J. T., Piazza, G. A., Han, E. K., Delohery, T. M., Li, H., Finn, T. S., Buttyan, R., Yamamoto, H., Sperl, G. J., Brendel, K., Gross, P. H., Pamukcu, R., and Weinstein, I. B. Sulindac derivatives inhibit growth and induce apoptosis in human prostate cancer cell lines. Biochem. Pharmacol., *58:* 1097–1107, 1999.

8. Gundersen, G. G., and Bulinski, J. C. Selective stabilization of microtubules oriented toward the direction of cell migration. Proc. Natl. Acad. Sci. USA, *85:* 5946–5950, 1988.

9. Cook, T. A., Nagasaki, T., and Gundersen, G. G. Rho guanosine triphosphatase mediates the selective stabilization of microtubules induced by lysophosphatidic acid. J. Cell Biol., *141:* 175–185, 1998.

10. Gundersen, G. G., Kreitzer, G., Cook, T., and Liao, G. Microtubules as determinants of cellular polarity. Biol. Bull., *194:* 358–360, 1998.

11. Jordan, M. A., and Wilson, L. Kinetic analysis of tubulin exchange at microtubule ends at low vinblastine concentrations. Biochemistry, *29:* 2730–2739, 1990.

12. Derry, W. B., Wilson, L., and Jordan, M. A. Substoichiometric binding of Taxol suppresses microtubule dynamics. Biochemistry, *34:* 2203–2211, 1995.

13. Schiff, P. B., and Horwitz, S. B. Taxol assembles tubulin in the absence of exogenous guanosine 5′-triphosphate or microtubule-associated proteins. Biochemistry, *20:* 3247–3252, 1981.

14. Jha, M. N., Bamburg, J. R., and Bedford, J. S. Cell cycle arrest by Colcemid differs in human normal and tumor cells. Cancer Res., *54:* 5011–5015, 1994.

15. Ince, P., Elliott, K., Appleton, D. R., Moorghen, M., Finney, K. J., Sunter, J. P., Harris, A. L., and Watson, A. J. Modulation by verapamil of vincristine pharmacokinetics and sensitivity to metaphase arrest of the normal rat colon in organ culture. Biochem. Pharmacol., *41:* 1217–1225, 1991.

16. Barth, R. F. Rat brain tumor models in experimental neuro-oncology: the 9L, C6, T9, F98, RG2 (D74), RT-2 and CNS-1 gliomas. J. Neurooncol., *36:* 91–102, 1998.

17. Begemann, M., Kashimawo, S. A., Choi, Y. A., Kim, S., Christiansen, K. M., Duigou, G., Mueller, M., Schieren, I., Ghosh, S., Fabbro, D., Lampen, N. M., Heitjan, D. F., Schiff, P. B., Bruce, J. N., and Weinstein, I. B. Inhibition of the growth of glioblastomas by CGP 41251, an inhibitor of protein kinase C, and by a phorbol ester tumor promoter. Clin. Cancer Res., *2:* 1017–1030, 1996.

18. Venkatraj, V. S., Begemann, M., Sobrino, A., Bruce, J. N., Weinstein, I. B., and Warburton, D. Genomic changes in glioblastoma cell lines detected by comparative genomic hybridization. J. Neurooncol., *36:* 141–148, 1998.

19. Alonso, A., Li, S., and Warburton, P. E. Analysis of the structure and the function of the human centromere/kinetochore complex using immunofluorescence and the FISH to normal and variant centromeres. *In:* E. J. M. Speel (ed.), Chromosome Analysis in Protocols. Totowa, NJ: Humana Press, in press.

20. Li, Y., and Benezra, R. Identification of a human mitotic checkpoint gene: *hsMAD2*. Science (Wash. DC), *274:* 246–248, 1996.

21. Kilmartin, J. V., Wright, B., and Milstein, C. Rat monoclonal antitubulin antibodies derived by using a new nonsecreting rat cell line. J. Cell Biol., *93:* 576–582, 1982.

22. Gundersen, G. G., Kalnoski, M. H., and Bulinski, J. C. Distinct populations of microtubules: tyrosinated and nontyrosinated α tubulin are distributed differently *in vivo*. Cell, *38:* 779–789, 1984.

23. Doxsey, S. J., Stein, P., Evans, L., Calarco, P. D., and Kirschner, M. Pericentrin, a highly conserved centrosome protein involved in microtubule organization [see comments]. Cell, *76:* 639–650, 1994.

24. Davis, F. M., Tsao, T. Y., Fowler, S. K., and Rao, P. N. Monoclonal antibodies to mitotic cells. Proc. Natl. Acad. Sci. USA, *80:* 2926–2930, 1983.

25. Kuang, J., Zhao, J., Wright, D. A., Saunders, G. F., and Rao, P. N. Mitosis-specific monoclonal antibody MPM-2 inhibits *Xenopus* oocyte maturation and depletes maturation-promoting activity. Proc. Natl. Acad. Sci. USA, *86:* 4982–4986, 1989.

26. Westendorf, J. M., Rao, P. N., and Gerace, L. Cloning of cDNAs for M-phase phosphoproteins recognized by the MPM2 monoclonal antibody and determination of the phosphorylated epitope. Proc. Natl. Acad. Sci. USA, *91:* 714–718, 1994.

27. Grafi, G. Cell cycle regulation of DNA replication: the endoreduplication perspective. Exp. Cell Res., *244:* 372–378, 1998.

28. Li, Y., Gorbea, C., Mahaffey, D., Rechsteiner, M., and Benezra, R. MAD2 associates with the cyclosome/anaphase-promoting complex and inhibits its activity. Proc. Natl. Acad. Sci. USA, *94:* 12431–12436, 1997.

29. Glotzer, M. Mitosis: don't get mad, get even. Curr. Biol., *6:* 1592–1594, 1996.

30. Waters, J. C., Chen, R. H., Murray, A. W., Gorbsky, G. J., Salmon, E. D., and Nicklas, R. B. Mad2 binding by phosphorylated kinetochores links error detection and checkpoint action in mitosis. Curr. Biol., *9:* 649–652, 1999.

31. Straight, A. F. Cell cycle: checkpoint proteins and kinetochores. Curr. Biol., *7:* R613–R616, 1997.

32. Rudner, A. D., and Murray, A. W. The spindle assembly checkpoint. Curr. Opin. Cell Biol., *8:* 773–780, 1996.

33. Waters, J. C., Chen, R. H., Murray, A. W., and Salmon, E. D. Localization of Mad2 to kinetochores depends on microtubule attachment, not tension. J. Cell Biol., *141:* 1181–1191, 1998.

34. Dhamodharan, R., Jordan, M. A., Thrower, D., Wilson, L., and Wadsworth, P. Vinblastine suppresses dynamics of individual microtubules in living interphase cells. Mol. Biol. Cell, *6:* 1215–1229, 1995.

35. Webster, D. R., Gundersen, G. G., Bulinski, J. C., and Borisy, G. G. Differential turnover of tyrosinated and detyrosinated microtubules. Proc. Natl. Acad. Sci. USA, *84:* 9040–9044, 1987.

36. Gundersen, G. G., and Bulinski, J. C. Microtubule arrays in differentiated cells contain elevated levels of a post-translationally modified form of tubulin. Eur. J. Cell Biol., *42:* 288–294, 1986.

37. Gundersen, G. G., Kim, I., and Chapin, C. J. Induction of stable microtubules in 3T3 fibroblasts by TGF-β and serum. J. Cell Sci., *107:* 645–659, 1994.

38. Gundersen, G. G., and Cook, T. A. Microtubules and signal transduction. Curr. Opin. Cell Biol., *11:* 81–94, 1999.

39. Thompson, W. J., Piazza, G. A., Li, H., Liu, L., Fetter, J., Zhu, B., Sperl, G., Ahnen, D., and Pamukcu, R. Exisulind induction of apoptosis involves guanosine 3′,5′-cyclic monophosphate phosphodiesterase inhibition, protein kinase G activation, and attenuated β-catenin. Cancer Res., *60:* 3338–3342, 2000.

40. Soh, J. W., Mao, Y., Kim, M. G., Pamukcu, R., Li, H., Piazza, G. A., Thompson, W. J., and Weinstein, I. B. Cyclic GMP mediates apoptosis induced by sulindac derivatives via activation of c-Jun NH2-terminal kinase 1. Clin. Cancer Res., *6:* 4136–4141, 2000.

41. Denninger, J. W., Schelvis, J. P., Brandish, P. E., Zhao, Y., Babcock, G. T., and Marletta, M. A. Interaction of soluble guanylate cyclase with YC-1: kinetic and resonance Raman studies. Biochemistry, *39:* 4191–4198, 2000.

42. Keates, R. A., and Mason, G. B. Inhibition of microtubule polymerization by the tubulin-colchicine complex: inhibition of spontaneous assembly. Can. J. Biochem., *59:* 361–370, 1981.

43. Hanif, R., Pittas, A., Feng, Y., Koutsos, M. I., Qiao, L., Staiano-Coico, L., Shiff, S. I., and Rigas, B. Effects of nonsteroidal anti-inflammatory drugs on proliferation and on induction of apoptosis in colon cancer cells by a prostaglandin- independent pathway. Biochem. Pharmacol., *52:* 237–245, 1996.

44. Thompson, H. J., Briggs, S., Paranka, N. S., Piazza, G. A., Brendel, K., Gross, P. H., Sperl, G. J., Pamukcu, R., and Ahnen, D. J. Inhibition of mammary carcinogenesis in rats by sulfone metabolite of sulindac. J. Natl. Cancer Inst. (Bethesda), *87:* 1259–1260, 1995.

45. Wilson, L., and Jordan, M. A. Pharmacological probes of microtubule function. *In:* J. S. Hyams and C. W. Lloyd (eds.), Microtubules, Vol. 13, pp. 59–83. New York: Wiley-Liss, 1994.

46. Mikhailov, A., and Gundersen, G. G. Relationship between microtubule dynamics and lamellipodium formation revealed by direct imaging of microtubules in cells treated with nocodazole or Taxol. Cell Motil. Cytoskeleton, *41:* 325–340, 1998.

47. Andreu, J. M., Perez-Ramirez, B., Gorbunoff, M. J., Ayala, D., and Timasheff, S. N. Role of the colchicine ring A and its methoxy groups in the binding to tubulin and microtubule inhibition. Biochemistry, *37:* 8356–8368, 1998.

48. Gajate, C., Barasoain, I., Andreu, J. M., and Mollinedo, F. Induction of apoptosis in leukemic cells by the reversible microtubule- disrupting agent 2-methoxy-5-(2′,3′,4′-trimethoxyphenyl)-2,4,6-cycloheptatrien-1-one: protection by Bcl-2 and Bcl-X(L) and cell cycle arrest. Cancer Res., *60:* 2651–2659, 2000.